RSC Advances

PAPER

View Article Online
View Journal | View Issue

Cite this: *RSC Adv.*, 2019, **9**, 29779

Understanding the structural transformation of carbon black from solid spheres to hollow polyhedra during high temperature treatment

Chengwei Fan,[a] Yifan Liu,[b] Jiayao Zhu,[a] Luxiang Wang,[a] Xiaohong Chen,[b] Su Zhang,*[a] Huaihe Song *[b] and Dianzeng Jia *[a]

Received 28th August 2019
Accepted 16th September 2019

DOI: 10.1039/c9ra06828g

rsc.li/rsc-advances

Understanding the structural transformation of carbon black during high temperature treatment and the underlying mechanism are very important because of the correlation with nanocarbon species such as fullerenes and carbon onions. Herein, we find that carbon black nanoparticles exhibit a solid skin–core structure constructed from small graphene flakes. The skin shows a more ordered structure than the core. During heating treatment in an inert atmosphere, the small graphene flakes coalesce together to form large-area lamellae at 1600 °C. Then, the solid spherical nanoparticles completely transform to hollow polyhedra at 1800 °C with significantly improved crystallinity. What's more, the inner cores of carbon black can be removed through simple oxidation in air, demonstrating that the cores are more disordered and reactive than the skin. Accordingly, the structural transformation mechanism is ascribed to well-ordered graphitic shells being preferentially formed by coalescing ordered small graphene flakes in the skin region of carbon black nanoparticles. The multilocular hollow structure is subsequently formed by reconstruction of highly disordered and twisted inner cores in a confined space.

Introduction

Carbon black (CB) is a traditional carbon material which has been widely used in many industrial manufacturing processes, such as those of rubbers, plastics, catalyst supports, pigments, and electrodes.[1–5] It contains over 97–99% elemental carbon depending on the manufacturing process.[3] Generally, CB has good thermal and electrical conductivity, low density, high specific surface area, and high mechanical strength. These properties are closely related to its unique structure and surface properties. The structural characteristics of CB have been investigated for more than eighty years by many techniques such as X-ray diffraction (XRD),[5–9] Raman spectroscopy,[10,11] electron microscopy,[12–14] and electron energy loss spectroscopy.[15] Some generally accepted results and mechanisms have been obtained from the previous studies. From the high resolution transmission electron microscopy (HRTEM) and simulation results,[1,12–17] the primary CB nanoparticle is considered as a gradient skin–core structure constructed from small graphene flakes as building blocks. The small graphene layers generally arrange according to a concentric or turbulent-like feature. But this arrangement trend gradually diminishes towards the particle center. As a result, the small graphene flakes are densely packed to form relative ordered skin, while loose stacked to form disordered and twisted cores.[1,12,17] Although CB shows an overall amorphous nature from the XRD measurement, it cannot be considered as globally amorphous because they have large numbers of small crystalline domains mainly distributed in the skin region.[10,11]

CB is commonly prepared by pyrolysis of carbon-rich precursors such as natural gas, pitch, and aromatic heavy oil at high temperature above 1200 °C. The possible CB formation mechanism was proposed by Donnet *et al.*[18] and Bourrat *et al.*[19] It involves three stages: (I) nucleation, transformation of gaseous hydrocarbon precursor to small solid or liquid carbon nucleus at high temperature; (II) growth (aggregation), deposition of carbonaceous components on the nucleus to form 10–50 nm spherical particles; and (III) agglomeration, coalescence of the as-formed nanoparticles along with the further deposition to form a multilocular structure.[3,17] Therefore, formation of the skin–core structure is attributed to: (I) in the nucleation stage, hydrocarbon molecules undergo complex decomposition and polymerization processes, resulting in the formation of twisted polycyclic aromatic hydrocarbons. These polycyclic aromatic hydrocarbons loose stack together to form primary solid carbon nucleus (cores) with the diameter of several nanometers. (II) In the later growth stage, pyrolytic carbon deposition continuously occurs on the nucleus (cores), resulting

[a]*Key Laboratory of Energy Materials Chemistry, Ministry of Education, Key Laboratory of Advanced Functional Materials, Autonomous Region, Institute of Applied Chemistry, Xinjiang University, Urumqi, 830046, P. R. China. E-mail: suzhangs@163.com; jdz@xju.edu.cn*

[b]*State Key Laboratory of Chemical Resource Engineering, Beijing Key Laboratory of Electrochemical Process and Technology for Materials, Beijing University of Chemical Technology, Beijing, 100029, P. R. China. E-mail: songhh@mail.buct.edu.cn*

in the formation of relatively dense and ordered carbon skin. Therefore, the outer carbon skin in CB shows higher crystallinity than that of inner carbon core.

Thermal treatment is the most common route to modulate the structure and property of CB.[20–24] For example, the crystallinity and electric conductivity can be significantly improved by high temperature graphitization.[7,10,21] Interestingly, a structural transformation of carbon nanoparticles from solid nanospheres to hollow nano-polyhedra through high temperature treatment has been realized in the previous works.[20–26] But clear observation and deep investigation of this transformation process are still absent so far. In particular, the structural transformation process at different temperatures is not revealed. Herein, a typical N330 CB was thermal treated at different temperatures ranging from 1500 to 2800 °C in inert atmosphere, and a general structural transformation from solid spherical nanoparticles to hollow nano-polyhedra is investigated in detail. The transformation mechanism is deduced to the coalescence and reconstruction of small graphene flakes in the skin and core of CB nanoparticles. Our work can help to understand the structure of CB during high temperature treatment, which may also extends to other nanocarbons such as fullerenes and carbon onions.

Experimental section

The commercially available N330 CB was chosen as an exemplification. N330 CB were treated at 1500, 1600, 1800, 2000, and 2800 °C for 1 h in Ar atmosphere. The obtained samples were marked as "N330-temperature". For air oxidation, N330 CB was put into a corundum crucible and heated at 430 °C for 6 h in air atmosphere in a muffle oven. The sample is named as AO-N330. The structure was measured by HRTEM (JEOL-2100). The XRD measurement was recorded on a Rigaku D/max2500B2+/PCX system operating at 40 kV and 20 mA using Cu Kα radiation. The Raman spectroscopy was characterized using 532 nm laser (Aramis, Jobin Yvon). The Fourier-transform infrared spectroscopy (FT-IR) was recorded on a Nicolet Nexus 670 infrared spectrometer. The X-ray photoelectron spectroscopy (XPS) was recorded on an Escalab 250 spectrometer using monochromatic Al Kα (1486.6 eV) X-ray source with 30 eV pass energy in 0.5 eV step over an area of 650 × 650 μm to the sample.

Results and discussion

The TEM images of the samples in low magnification are given in Fig. 1 to understand the general structural transformation of CB. The primary N330 CB nanoparticles exhibit a solid spherical morphology. This structure is barely changed before 1800 °C (Fig. 1c). Thereafter, all of the nanoparticles are gradually transformed to hollow polyhedra (Fig. 1d–f). The HRTEM images are given in Fig. 2 for clear understanding. The turbulent skin–core structure of N330 CB nanoparticles is clearly identified in Fig. 2a. The skin region is constructed by densely packed small graphene flakes arranged in a concentric feature, while the core region is formed by disordered and twisted carbon flakes.[1,12–17] The skin–core structure remains with slight

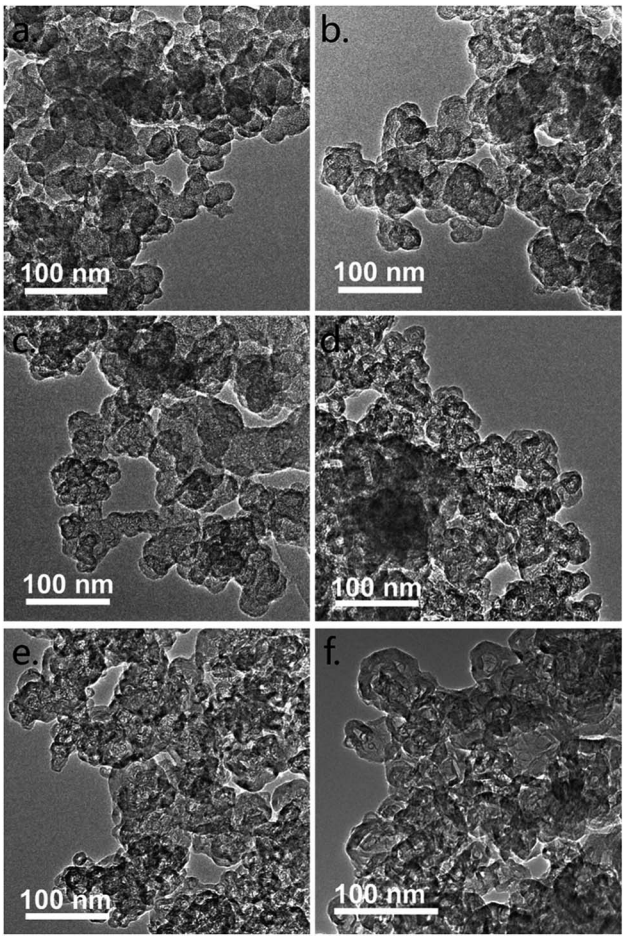

Fig. 1 TEM images of (a) N330, (b) N330-1500, (c) N330-1600, (d) N330-1800, (e) N330-2000, and (f) N330-2800.

coalescing of the small graphene flakes in the skin for N330-1500 (Fig. 2b). When the treated temperature raised to 1600 °C, the small graphene flakes in CB nanoparticles continuously coalesce together, leading to the formation of large area graphene lamellas in the whole N330-1600 nanoparticles (Fig. 2c). But it should be noticed that the structures in the skin and core regions are very different. The graphene flakes are packed densely to form a multilayer structure in the skin region. By contrast, although the graphene flakes in core region are enlarged due to the coalescence, they still exhibit a highly disordered and twisted structure observed from Fig. 2c. The solid spherical nanoparticles thereafter are fully transformed to hollow nano-polyhedra with much ordered and compact multilayer graphitic shells at the temperature above 1800 °C (Fig. 2d–f). Several thin layer graphitic carbon onions are observed inside the inner space of the nano-polyhedra. And these nano-onions are partially merged into the outer graphitic shells, resulting in the multiple core structure (Fig. 2d–f).[21,23,25,26] The structural transformation model according to the HRTEM observation is given in Fig. 2g.

The characteristic (002) and (100) diffraction peaks are clearly identified at *ca.* 26 and 43° in the XRD patterns of the samples (Fig. 3a). A broad and dispersive peak located at 24.5°

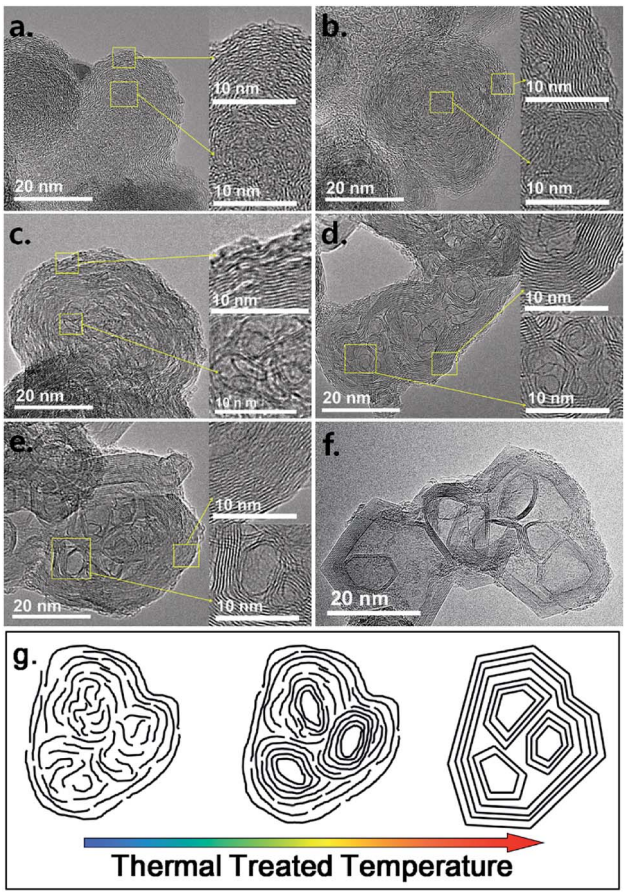

Fig. 2 HRTEM images of (a) N330, (b) N330-1500, (c) N330-1600, (d) N330-1800, (e) N330-2000, and (f) N330-2800; (g) structural transformation model according to the HRTEM images.

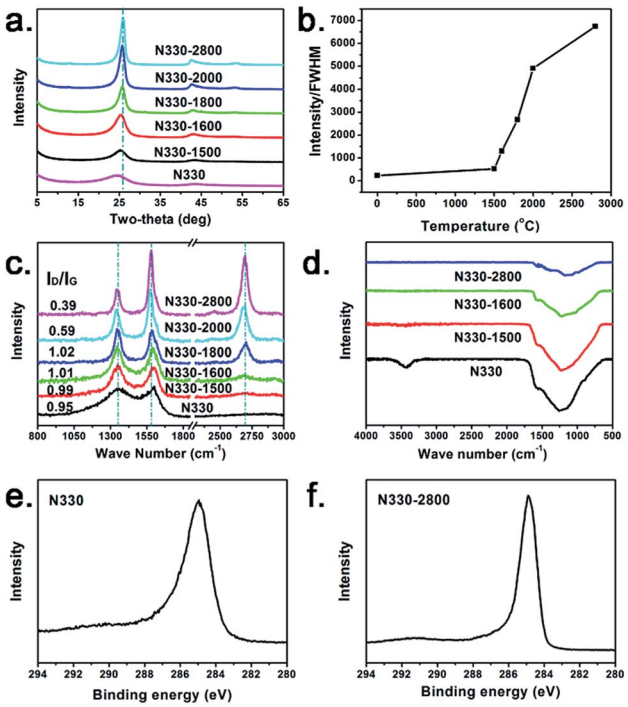

Fig. 3 (a) XRD patterns, (b) the ratio of the intensity to the full width at half maximum (FWHM) of the (002) peaks at *ca.* 26°, (c) Raman, and (d) FT-IR spectra of the obtained samples. XPS C_{1s} curves of (e) N330 and (f) N330-2800.

in the spectrum of N330 CB indicates its amorphous feature.[5–9] With the rising of heating temperature, the (002) peak is gradually shifted to high degree of 26°. And the diffraction peaks are significantly sharped, demonstrating the significantly improved crystallinity. The ratio of the intensity to the full width at half maximum (FWHM) of the (002) peak located at *ca.* 26° of each sample is used to express the crystallinity of each sample (Fig. 3b).[27] The slight crystallinity increase from N330 to N330-1500 is due to the partially coalesced graphene flakes in the skin region, as observed from the HRTEM image in Fig. 2b. The crystallinity of the samples shows a rapid increase after 1600 °C, reaching to a plateau above 2000 °C. This indicates the coalescence of small graphene flakes and gradual formation of large-area ordered graphitic structure with the increasing of treating temperature, which is in accordance with the HRTEM observation in Fig. 2.

The peaks located at *ca.* 1350 and 1580 cm^{-1} in the Raman spectra (Fig. 3c) are the D- and G-band, respectively. The broad and dispersive G band and the intensive D band of the N330 CB indicate that it is constructed by large numbers of micro-crystallites separated by a considerable amount of amorphous regions.[10,11] The D-band are weakened and the G-band are sharpened along with the rising of treating temperature, also demonstrating the formation of large area graphitic conjugated structure by coalescence and merging of the small graphene fragments in N330 CB.[10,28] Moreover, the 2D-band located at 2695 cm^{-1} can be detected in N330-1600 and becomes intensive and sharp subsequently. Corresponding to the significantly increased crystallinity from the XRD result, this indicates the arising of strong interlayer interaction between the graphitic layers in the shell region of the nano-polyhedra.[29] N330 CB and its thermal treated samples shows the similar FT-IR characteristics (Fig. 3d). Common oxygen-bearing functional groups such as C–O–C, –OH, –C=O, and –COOH are not detected. The XPS C_{1s} curve of N330 CB is narrowed after high temperature treatment (Fig. 3e and f), indicating the multiple hybridized states of the carbon atoms (sp^2, sp^3 C, and defects) in the amorphous N330 CB skeleton are decreased along with the structural transformation to more ordered one.

It should be mentioned that the mass residual of N330 CB even after 2800 °C treatment is more than 97%, demonstrating that formation of hollow polyhedral structure is not due to removal of the inner cores. To deeply understand the structural transformation mechanism, we oxidized N330 CB at 430 °C in air atmosphere. We find that the solid spherical N330 nanoparticles are also transformed to hollow spherical nanoparticles (Fig. 4a and b) with the mass loss of nearly 50%. But this phenomenon is different in principle from the high temperature induced transformation. In accordance with the early study by Donnet *et al.*,[30] the hollow structure is due to etching and removal of the inner cores of N330 CB during air oxidation. The

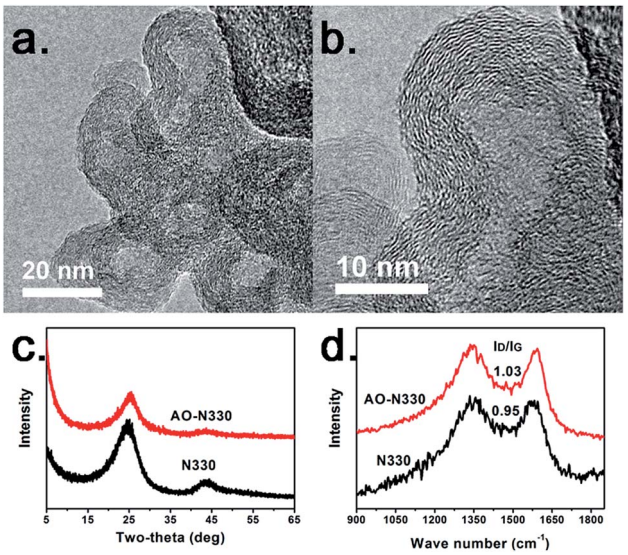

Fig. 4 (a) and (b) HRTEM images of the AO-N330, (c) XRD and (d) Raman patterns of N330 CB and AO-N330.

carbon shell still shows a concentric fashion (Fig. 4b). The XRD and Raman patterns given in Fig. 4c and d indicate that AO-N330 still shows a low crystallinity and a high defect density, which is similar as those of N330 CB. The coalescence or reconstruction of small graphene flakes is barely occurred at the relative low temperature of 430 °C. The aforementioned results not only provide a direct evidence for the skin–core structure of CB nanoparticles, but also demonstrate that the graphene flakes of the core regions are more disordered and twisted than those of the skin regions because the cores are more reactive for air oxidation.

From the discussion above, the structural transformation mechanism is proposed (model shown in Fig. 1g). First, we should review the formation process of CB. The hydrocarbon precursors undergo decomposition and condensation under high fabrication temperature, resulting in the formation of polycyclic aromatic hydrocarbons as nucleuses (cores). These nucleuses (cores) are of a highly twisted and defective structure, and may stack loosely with each other because of the short liquid-maintaining time at high temperature. Thereafter, pyrolytic deposition takes place on these nucleuses to form a relatively dense and ordered pyrolytic carbon skin. Because of continues aggregation and deposition, CB nanoparticles tend to form as a skin–core structure.[3,17–19] When these nanoparticles undergo a high temperature treatment, well ordered graphitic skin is preferentially formed by easy coalescence and reconstruction of the small graphene flakes in the dense and ordered pyrolytic carbon skin.[31,32] But large-sized ordered graphitic lamellas are hardly formed in the core region because the graphene flakes show a highly disordered and twisted structure in a confined space. At higher temperature, these twisted graphene flakes are transformed to onion-like carbons, leading to the formation of a multilocular hollow structure.[31,32] The proposed mechanism is in well accordance with our experimental results. What's more, from the energy point of view, the small graphene flakes tend to coalesce together with the rising of treating temperature to diminish high energy edges, crystal boundary, and defects. Concentric arranged graphene flakes in the skin region of CB nanoparticles therefore, are easily transformed to multilayer stacked graphitic shells. But because of the steric hindrance effect in a confined space, the highly twisted graphene flakes in the core region are more difficult to rearrange. At higher treating temperature, these highly twisted graphene flakes coalesce and tend to flattened in a confined space to form graphitic carbon onions to further reduce the systematic energy. As a result, the solid spherical CB nanoparticles are transformed to hollow nano-polyhedra through high temperature thermal treatment.

Conclusions

CB nanoparticles show a structural transformation from solid spherical nanospheres to hollow nano-polyhedra during high temperature thermal treatment. CB nanoparticles have a skin–core structure constructed by small graphene flakes. The graphene flakes are densely packed in the skin region and disordered and twisted in the core region. We found that the small graphene flakes were coalesced together at 1600 °C. Then CB solid spheres were completely transformed to polyhedra at 1800 °C. By air oxidation, we proved that the cores were more reactive than the skin. Therefore, the structural transformation mechanism is ascribed to that the small graphene flakes coalesce together to form large graphene lamellas, leading to a densely packed graphitic skin and several twisted cores. Subsequently, a multilocular hollow structure is formed by reconstruction of carbons in a confined core region.

Conflicts of interest

There are no conflicts to declare.

Acknowledgements

This work was financially supported by the National Natural Science Foundation of China (No. 51672021, U1610252, and 51702275), the Scientific Research Program of the Higher Education Institution of Xinjiang (XJEDU2017S003), Xinjiang Tianchi Doctoral Project, and the Fund of the State Key Laboratory of Chemical Resource Engineering (No. CRE-2017-C-201).

Notes and references

1 S. Ban, K. Malek, C. Huang and Z. Liu, *Carbon*, 2011, **49**, 3362–3370.
2 M. Wissler, Graphite and carbon powders for electrochemical applications, *J. Power Sources*, 2006, **156**, 142–150.
3 F. Fabry, G. Flamant and L. Fulcheri, Carbon black processing by thermal plasma analysis of the particle formation mechanism, *Chem. Eng. Sci.*, 2001, **56**, 2123–2132.
4 C. Liu, A. B. Walters and M. A. Vannice, *Carbon*, 1995, **33**, 1699–1708.

5 T. Ungár, J. Gubicza, G. Ribárik, C. Pantea and T. W. Zerda, *Carbon*, 2002, **40**, 929–937.
6 B. E. Warren, *J. Chem. Phys.*, 1934, **2**, 551–555.
7 H. T. Pinnick, *J. Chem. Phys.*, 1952, **20**, 756–757.
8 L. Alexander and S. R. Darin, *J. Chem. Phys.*, 1955, **23**, 594–595.
9 T. Ungár, J. Gubicza, G. Tichy, C. Pantea and T. W. Zerda, *Composites, Part A*, 2005, **36**, 431–436.
10 T. Gruber, T. W. Zerda and M. Gerspacher, *Carbon*, 1994, **32**, 1377–1382.
11 T. Jawhari, A. Roid and J. Casado, *Carbon*, 1995, **33**, 1561–1565.
12 D. Ugarte, *Z. Phys. D: At., Mol. Clusters*, 1993, **26**, 150–152.
13 C. Jäger, T. Henning, R. Schlögl and O. Spillecke, *J. Non-Cryst. Solids*, 1999, **258**, 161–179.
14 W. Zhu, D. E. Miser, W. G. Chan and M. R. Hajaligol, *Carbon*, 2004, **42**, 1841–1845.
15 T. Pichler, *Phys. Rev. B: Condens. Matter Mater. Phys.*, 2001, **63**, 155415.
16 I. Morozov, B. Lauke and G. Heinrich, *Comput. Mater. Sci.*, 2010, **47**, 817–825.
17 F. Cataldo and M. A. Pontier-Johnson, *Fullerenes, Nanotubes, Carbon Nanostruct.*, 2002, **10**, 1–14.
18 J. B. Donnet, R. C. Bansal and M. J. Wang, *Carbon blacks: Science and technology*, CRC Press, 1993.
19 X. Bourrat, Structure in carbons and carbon artifacts, in *Sciences of carbon materials*, ed. H. Marsh and F. Rodriguez-Reinoso, Universidad de Alicante, Alicante, 2000, pp. 194–196.
20 W. D. Schaeffer, W. R. Smith and M. H. Polley, *Ind. Eng. Chem.*, 1953, **45**, 1721–1725.
21 W. A. de Heer and D. Ugarte, *Chem. Phys. Lett.*, 1993, **207**, 480–486.
22 W. M. Hess, L. L. Ban, F. J. Eckert and V. Chirico, *Rubber Chem. Technol.*, 1968, **41**, 356–372.
23 D. Ugarte, *Carbon*, 1994, **32**, 1245–1248.
24 W. Lian, H. Song, X. Chen, L. Li, J. Huo, M. Zhao and G. Wang, *Carbon*, 2008, **46**, 525–530.
25 Y. Z. Jin, Y. J. Kim, C. Gao, Y. Q. Zhu, A. Huczko, M. Endo and H. W. Kroto, *Carbon*, 2006, **44**, 724–729.
26 F. Cataldo, *Fullerene Sci. Technol.*, 2000, **8**, 105–112.
27 S. Zhang, Y. Cui, B. Wu, R. Song, H. Song, J. Zhou, X. Chen, J. Liu and L. Cao, *RSC Adv.*, 2014, **4**, 505–509.
28 E. B. Barros, N. S. Demir, A. G. S. Filho, J. M. Filho, A. Jorio, G. Dresselhaus and M. S. Dresselhause, *Phys. Rev. B: Condens. Matter Mater. Phys.*, 2005, **71**, 165422.
29 L. G. Cançado, K. Takai, T. Enoki, M. Endo, Y. A. Kim, H. Mizusaki, N. L. Spezial, A. Jorio and M. A. Pimenta, *Carbon*, 2008, **46**, 272–275.
30 J. B. Donnet, J. Schultz and A. Eckhardt, *Carbon*, 1968, **6**, 781–788.
31 A. Oberlin, *Carbon*, 1984, **22**, 521–541.
32 C. Tomas, I. Suarez-Martinez, F. Vallejos-Burgos, M. J. López, K. Kaneko and N. A. Marks, *Carbon*, 2017, **119**, 1–9.